

SketchANIMAR: Sketch-based 3D Animal Fine-Grained Retrieval

Trung-Nghia Le^{a,b}, Tam V. Nguyen^{b,c}, Minh-Quan Le^{b,a,b}, Trong-Thuan Nguyen^{b,a,b}, Viet-Tham Huynh^{b,a,b}, Trong-Le Do^{b,a,b}, Khanh-Duy Le^{b,a,b}, Mai-Khiem Tran^{b,a,b}, Nhat Hoang-Xuan^{b,a,b}, Thang-Long Nguyen-Ho^{b,a,b}, Vinh-Tiep Nguyen^{b,d,b}, Nhat-Quynh Le-Pham^{a,b}, Huu-Phuc Pham^{a,b}, Trong-Vu Hoang^{a,b}, Quang-Binh Nguyen^{a,b}, Trong-Hieu Nguyen-Mau^{b,a,b}, Tuan-Luc Huynh^{b,a,b}, Thanh-Danh Le^{a,b}, Ngoc-Linh Nguyen-Ha^{a,b}, Tuong-Vy Truong-Thuy^{a,b}, Truong Hoai Phong^{a,b}, Tuong-Nghiem Diep^{a,b}, Khanh-Duy Ho^{a,b}, Xuan-Hieu Nguyen^{a,b}, Thien-Phuc Tran^{a,b}, Tuan-Anh Yang^{a,b}, Kim-Phat Tran^{a,b}, Nhu-Vinh Hoang^{a,b}, Minh-Quang Nguyen^{a,b}, Hoai-Danh Vo^{a,b}, Minh-Hoa Doan^{a,b}, Hai-Dang Nguyen^{b,a,b}, Akihiro Sugimoto^{b,e}, Minh-Triet Tran^{b,a,b,*}

^aUniversity of Science, VNU-HCM, Ho Chi Minh City, Vietnam

^bVietnam National University, Ho Chi Minh City, Vietnam

^cUniversity of Dayton, Ohio, U.S.

^dUniversity of Information Technology, VNU-HCM, Ho Chi Minh City, Vietnam

^eNational Institute of Informatics, Tokyo, Japan

ARTICLE INFO

Article history:

Received April 13, 2023

3D object retrieval, fine-grained retrieval, and animal models.

ABSTRACT

The retrieval of 3D objects has gained significant importance in recent years due to its broad range of applications in computer vision, computer graphics, virtual reality, and augmented reality. However, the retrieval of 3D objects presents significant challenges due to the intricate nature of 3D models, which can vary in shape, size, and texture, and have numerous polygons and vertices. To this end, we introduce a novel SHREC challenge track that focuses on retrieving relevant 3D animal models from a dataset using sketch queries and expedites accessing 3D models through available sketches. Furthermore, a new dataset named ANIMAR was constructed in this study, comprising a collection of 711 unique 3D animal models and 140 corresponding sketch queries. Our contest requires participants to retrieve 3D models based on complex and detailed sketches. We receive satisfactory results from eight teams and 204 runs. Although further improvement is necessary, the proposed task has the potential to incentivize additional research in the domain of 3D object retrieval, potentially yielding benefits for a wide range of applications. We also provide insights into potential areas of future research, such as improving techniques for feature extraction and matching, and creating more diverse datasets to evaluate retrieval performance.

© 2023 Elsevier B.V. All rights reserved.

1. Introduction

The rapid development of 3D technologies produced a remarkable number of 3D objects. Consequently, 3D object retrieval has garnered considerable attention and is beneficial in real-life applications [1, 2, 3], including but not limited to video games, artistic pursuits, cinematography, and virtual reality.

Sketch-based 3D object retrieval aims to retrieve 3D models from a user's hand-drawn 2D sketch. Due to the innate intuitive appeal of freehand drawings, sketch-based 3D object retrieval has drawn a significant amount of attention and is being utilized in numerous critical applications such as 3D scene reconstruction [4, 5, 6], 3D geometry video retrieval [7, 8, 9], and 3D augmented/virtual reality entertainment [10, 11]. However, sketch-based 3D object retrieval poses a formidable challenge in 3D object retrieval research, primarily due to the large discrepancy between the 2D and 3D modalities: non-realistic 2D

*Corresponding author

e-mail: tmtriet@fit.hcmus.edu.vn (Minh-Triet Tran)

sketches differ significantly from their 3D counterparts and their respective views.

Several SHREC challenge tracks [12, 13, 14] have been organized to facilitate research on sketch-based 3D object retrieval. However, the existing datasets incorporated in these tracks primarily comprise generic objects with simplistic shapes and poses. To augment sketch-based 3D object retrieval research, we organize a new SHREC challenge track dedicated to *Sketch-based 3D ANIMAL model fine-grained Retrieval (SketchANIMAR)*¹. This track aims to retrieve relevant 3D animal models from a dataset using sketch queries and expedites accessing 3D models through available sketches. Previous SHREC challenge tracks have focused on a limited number of general object categories, often lacking realism. Our challenge track for SHREC 2023 is significantly more challenging and can simulate real-life scenarios more effectively than its predecessors.

First, conventional 3D object retrieval tasks consider only the object category, where the training and test samples are characterized by the same category settings. Consequently, features extracted from these methods are often optimized to fit the seen categories while lacking generalizability for unseen categories. Under such circumstances, the classification-based retrieval embedding learning methods become invalid in practice. Meanwhile, open-set 3D object retrieval can address this issue more effectively by dealing with unseen categories better. This technique involves training retrieval and representation models using seen-category 3D objects, with unseen-category 3D data subsequently used for retrieval. Nevertheless, our fine-grained retrieval task requires participants to conduct an accurate search to get 3D animal models whose shapes correspond to the query, necessitating consideration of unseen categories and poses (*cf.* Table 1). Compared to searching for 3D general objects of a given category, 3D animal model fine-grained retrieval poses a more significant challenge due to the substantial discrepancy in animal breeds and poses.

Second, participants in our track challenge must solve the considerable domain gap between sketches and 3D shapes when dealing with differently posed animals. Furthermore, human sketches on existing datasets tend to be semi-photorealistic and drawn by experts. In contrast, our dataset comprises more diverse sketches, including abstract sketches drawn by amateurs, semi-photorealistic sketches, and sketches in different styles (*cf.* Fig. 1). As such, this task proves significantly more challenging than conventional sketch-based object retrieval tasks. We anticipate that the sketch-based 3D animal fine-grained retrieval task can pave the way for a new research direction and exciting, practical applications.

The remainder of this paper is organized as follows. Section 2 provides an overview of related work. Section 3 presents the ANIMAR dataset and the evaluation measures used in this SHREC contest. Section 4 describes the participant statistics. In Section 5, the methods of the participating teams are presented. The results of the evaluation and an in-depth analysis of their performance are reported in Section 6. Finally, Section 7 concludes the paper and suggests directions for future work.

Table 1: SHREC challenge tracks for 3D object retrieval.

SHREC Challenge	Year	Query Type	Training Category	Testing Category
Hameed <i>et al.</i> [15]	2018	Image	Seen	Seen
Hameed <i>et al.</i> [16]	2019	Image	Seen	Seen
Li <i>et al.</i> [17]	2019	Image	Seen	Seen
Li <i>et al.</i> [18]	2020	Image	Seen	Seen
Feng <i>et al.</i> [19]	2022	Image	Seen	Unseen
Juefei <i>et al.</i> [20]	2018	Sketch	Seen	Seen
Juefei <i>et al.</i> [21]	2019	Sketch	Seen	Seen
Qin <i>et al.</i> [14]	2022	Sketch	Seen	Seen
SketchANIMAR	2023	Sketch	Unseen	Unseen

2. Related Work

To recover 3D objects from a database, content-based 3D object retrieval examines the visual contents of the objects, such as color, texture, form, and geometric aspects. Many tracks concentrating on similar problems have been held in previous SHREC competitions (see Table 1) to promote research on content-based 3D object retrieval.

Several SHREC tracks concentrate on retrieving 3D items in a database that resemble the 3D objects used as a query. The attractiveness of sketch-based 3D object retrieval, in particular, stems from the organic and intuitive quality of freehand sketches, and it has garnered a lot of attention in recent years. Juefei *et al.* [20, 21] promoted this intriguing study by organizing SHREC tracks of 2D scene sketch-based 3D scene retrieval. Domain adaptation algorithms were used, such as two-stream CNN with triplet loss, adversarial training, and different data augmentation techniques, to resolve the disagreement between two domains (*i.e.*, sketch and 3D object). In addition, a competition for sketch-based 3D form retrieval in the wild was conducted by Qin *et al.* [14], further advancing the task. They used a variety of 3D forms, including models created by scanning genuine things, as well as large-scale sketches created by amateur artists with a range of sketching abilities. Furthermore, technologies, such as point cloud learning and multi-view learning using various deep learning architectures, were created to emulate actual retrieval circumstances.

Sketch-based 3D object retrieval methods can be grouped into two categories: model-based and view-based approaches. Model-based methods commonly utilize 3D CNN to extract 3D shape features directly from the original 3D representations. In the view-based approach, 2D convolutional neural networks (CNN) are frequently used to analyze shape features from a set of 2D view projections.

Regarding the model-based approach, Furuya *et al.* [22] propose Deep Local Feature Aggregation Network (DLAN) which extracts rotation-invariant 3D local features and aggregates them in a single deep architecture. More concretely, the DLAN uses a set of 3D geometric features invariant to local rotation to characterize local 3D regions of a 3D model. The DLAN then compiles the set of features into a (global) rotation-invariant and compact feature for each 3D model. Furthermore, an Octree-based Convolutional Neural Network (O-CNN) [23] is also proposed for 3D shape analysis. O-CNN executes 3D

¹<https://aichallenge.hcmus.edu.vn/sketchanimar>

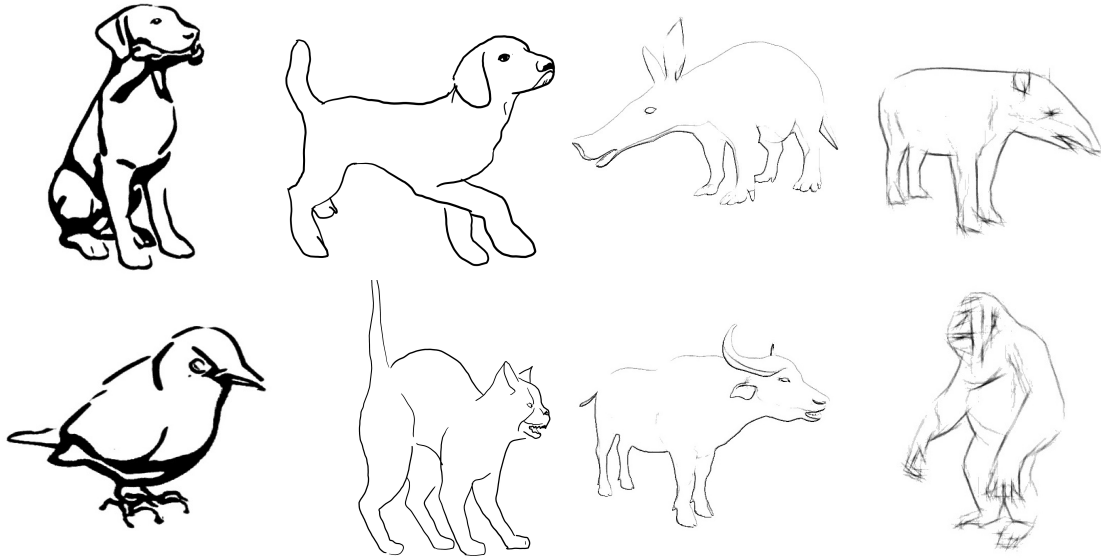


Fig. 1: Sketch ground-truth in ANIMAR dataset, including various sketch types.

CNN operations on the octants filled by the 3D shape surface using the average normal vectors of a 3D model sampled in the smallest leaf octants as input.

Concerning the view-based approach, Wang *et al.* [24] propose two Siamese Convolutional Neural Networks for the views and the sketches. Moreover, the loss function is designed for within-domain and cross-domain similarities. Similarly, two deep CNNs are proposed by Xie *et al.* [25] for deep feature extraction of sketches and 2D projections of 3D shapes. Next, the authors compute the Wasserstein barycenters of deep features of multiple projections of 3D shapes to form a barycentric representation. Last but not least, Multi-view Convolutional Neural Network (MVCNN) [26] creates a single, compact shape descriptor from data from multiple views of a 3D shape, which improves recognition performance.

In recent competitions of 3D Shape Retrieval Contests (SHREC) [27, 28, 14], teams achieving high performances follow the view-based approach.

3. Dataset and Evaluation

3.1. Dataset

In this competition, we constructed a new dataset, namely ANIMAR, which encompasses a corpus of 711 distinct 3D animal models along with 140 sketch queries.

We collected an impressive assemblage of 186 mesh models depicting over 50 diverse categories of animals. These models were diligently sourced from an array of publicly available online resources and video games, including the well-known Planet Zoo video game² [29]. The primary goal of our competition track was to simulate real-life scenarios in which users endeavor to identify and explore a diverse range of animal species. To achieve this, we purposely concealed categorical information during both the training and retrieval stages. Furthermore,

we refined our model database by generating a series of watertight mesh models by reducing the number of faces by ratios of 25%, 50%, and 75%, yielding a total of 525 models. Following the work of Douze *et al.* [30], our 3D animal model database is employed for both the training and retrieval phases.

We manually created 140 sketch images to describe 3D animal models. 74 sketches are aligned with their corresponding models in the database resulting in 297 pairs of query-model for training, while the remaining 66 sentences are utilized as queries, corresponding to 265 pairs of query-model, during the retrieval phase. Different from existing datasets, whose sketch ground-truth was semi-photorealistic and drawn by experts, our dataset comprises more diverse sketches, including abstract sketches drawn by amateurs, semi-photorealistic sketches, and sketches in different styles (*cf.* Fig. 1).

3.2. Evaluation Metrics

To evaluate the performance of different methods this track, the metrics used are:

- **Nearest Neighbor (NN)** evaluates top-1 retrieval accuracy.
- **Precision-at-10 (P@10)** is the ratio of relevant items in the top-10 returned results.
- **Normalized Discounted Cumulative Gain (NDCG)** is a measure of ranking quality defined as $\sum_{i=1}^p \frac{rel_i}{\log_2(i+1)}$, where p is the length of the returned rank list, and rel_i denotes the relevance of the i -th item.
- **Mean average precision (mAP)**, which is the area under the precision-recall curve, measures the precision of methods at different levels and then takes the average. mAP is calculated as $\frac{1}{r} \sum_{i=1}^r P(i)(R(i) - R(i - 1))$, where r is the number of retrieved relevant items, $P(i)$ and $R(i)$ are the precision and recall at the position of the i^{th} relevant item, respectively.

²<https://www.planetzoogame.com>

4. Participants

Eight groups legally participated in the SketchANIMAR challenge track, and 204 runs were submitted. Each group was given three weeks to complete the contest. They were registered to submit both their results and method description. The organizers did not participate in this challenge. The participant details are shown as follows:

- TikTorch team submitted by Nhat-Quynh Le-Pham, Huu-Phuc Pham, Trong-Vu Hoang, Quang-Binh Nguyen, and Hai-Dang Nguyen (*cf.* Section 5.2).
- THP team submitted by Truong Hoai Phong (*cf.* Section 5.3).
- Etinifni team submitted by Tuong-Nghiem Diep, Khanh-Duy Ho, Xuan-Hieu Nguyen, Thien-Phuc Tran, Tuan-Anh Yang, Kim-Phat Tran, Nhu-Vinh Hoang, and Minh-Quang Nguyen (*cf.* Section 5.4).
- V1olet team submitted by Trong-Hieu Nguyen-Mau, Tuan-Luc Huynh, Thanh-Danh Le, Ngoc-Linh Nguyen-Ha, and Tuong-Vy Truong-Thuy (*cf.* Section 5.5).
- DH team submitted by Hoai-Danh Vo and Minh-Hoa Doan (*cf.* Section 5.6).
- Nero team submitted by anonymous authors.
- K17hcmus team submitted by anonymous authors.
- Chongchongtrenobita team submitted by anonymous authors.

We remark that three anonymous teams did not agree to disclose their methods used in the competition. Therefore, we do not report the methods of these teams.

5. Methods

5.1. Overview of Submitted Solutions

For the representation of 3D objects, various techniques can be used, such as point cloud learning, or a set of random images of the object can be taken to serve as features. Each of these approaches is characterized by distinct mechanisms and tools. The features derived from these diverse methods exist in different spaces and thus require projection onto a common latent space to enable the representation learning process.

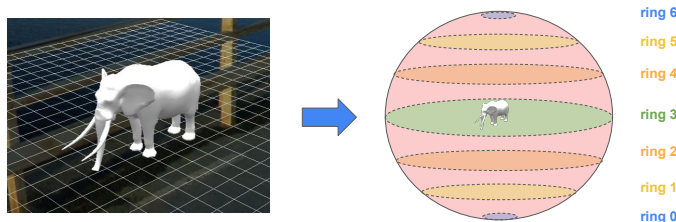


Fig. 2: 3D object represented as view sequences of 7 rings with 12 views on each ring. The chosen latitudes were 0 (the equator), ± 90 (the poles), and $\pm 30, \pm 60$.

All of the entries submitted to our track is based on view-based learning. This technique presents each 3D object through a sequence of ring images, as vividly portrayed in Fig. 2. These images are captured by strategically moving a camera around the object along a predetermined path, where each ring comprises a series of images. When the camera's trajectory is parallel to the ground plane in relation to the object, the multi-view method proves to be exceptionally effective, producing valuable images that aid in the process of extracting features for three-dimensional object representation.

To facilitate the retrieval task, TikTorch, THP, and Etinifni teams considered the problem as contrastive learning (as shown in Fig. 3). Meanwhile, V1olet team formulated the task as a classical classification problem (as depicted in Fig. 9). On the other hand, DH team directly extracted and compared non-deep learning features between sketch queries and generated sketches from 3D objects (see Fig. 10).

5.2. TikTorch Team

5.2.1. Proposed Contrastive Learning Solution

To retrieve 3D objects from sketch queries, they propose a contrastive learning framework where embedding vectors of 3D objects and 2D sketches are learned. The embedding vectors of similar objects and sketches should be closer to each other and vice versa.

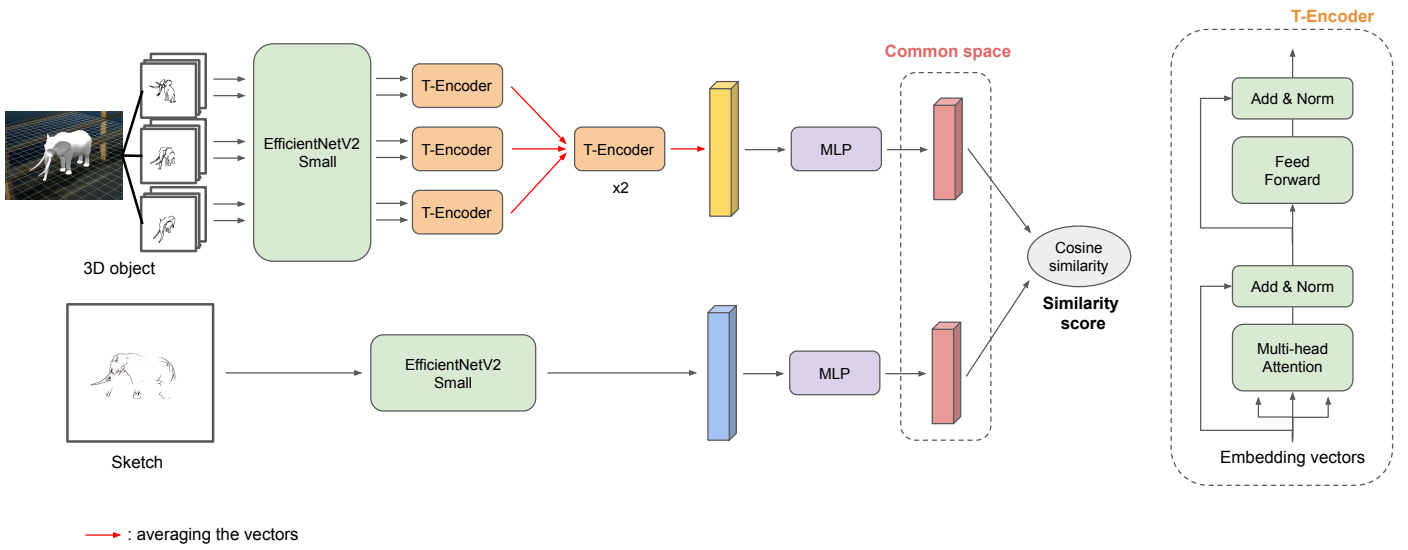
The overall architecture of their method is presented in Fig. 3a, containing two separate feature extractors for 3D objects and sketch images. The extracted feature vectors are then embedded in the common vector space by two Multi-layer Perceptron (MLP) networks. The contrastive loss used for simultaneous learning of the parameters for models is a customized version of Normalized Temperature-scaled Cross Entropy Loss (NT-Xent) [31].

Sketch feature extractor. To extract the features of sketch images, they fine-tune EfficientNetV2-Small [32] pretrained on ImageNet dataset [33]. The models in the EfficientNetV2 family reduce the parameter size significantly while maintaining competitive accuracy on many datasets, which is desirable for simple images, especially sketch images.

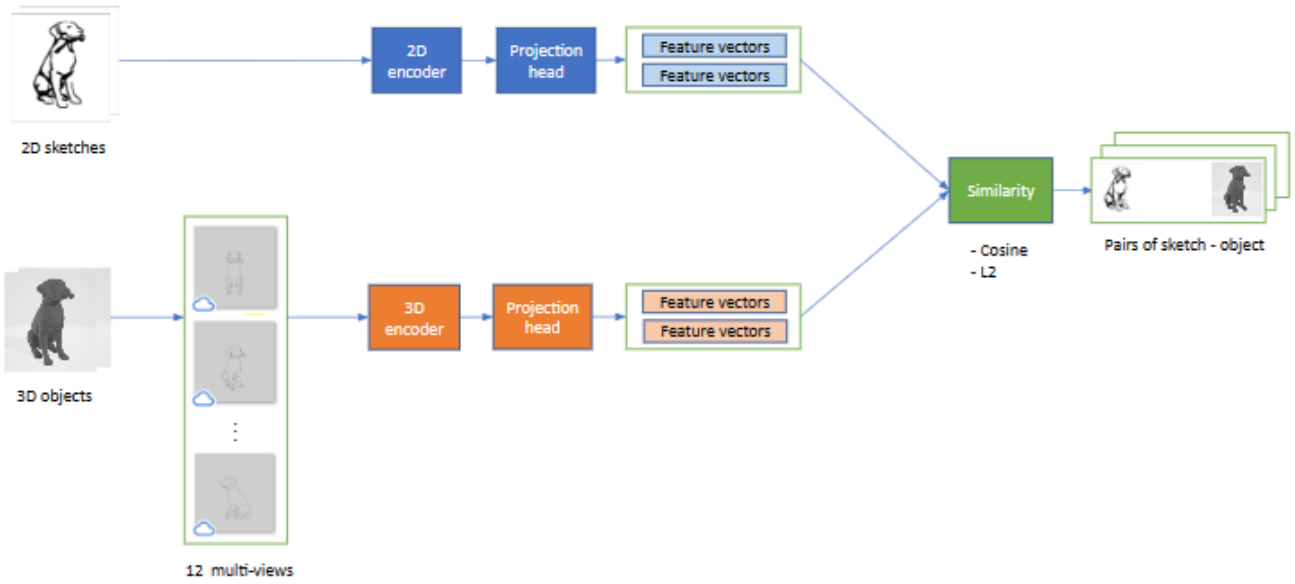
3D object feature extractor. Each 3D object is represented as a set of 3 rings and each ring contains 12 images. The 3D object feature extractor has 2 main phases: extracting the features of each ring (ring extractor) and combining the features of 3 rings to obtain the features of the object.

In the ring extractor, they also fine-tune EfficientNetV2-Small [32], similar to the sketch feature extractor module, to extract the features of 12 images of each ring. These 12 feature vectors then go through an encoder block called T-Encoder [34] to learn the relationship between images in the same ring to decide which image is important in the current ring and which image is not. After that, they combine these vectors together by simply calculating the average of them to get a single feature vector for each ring.

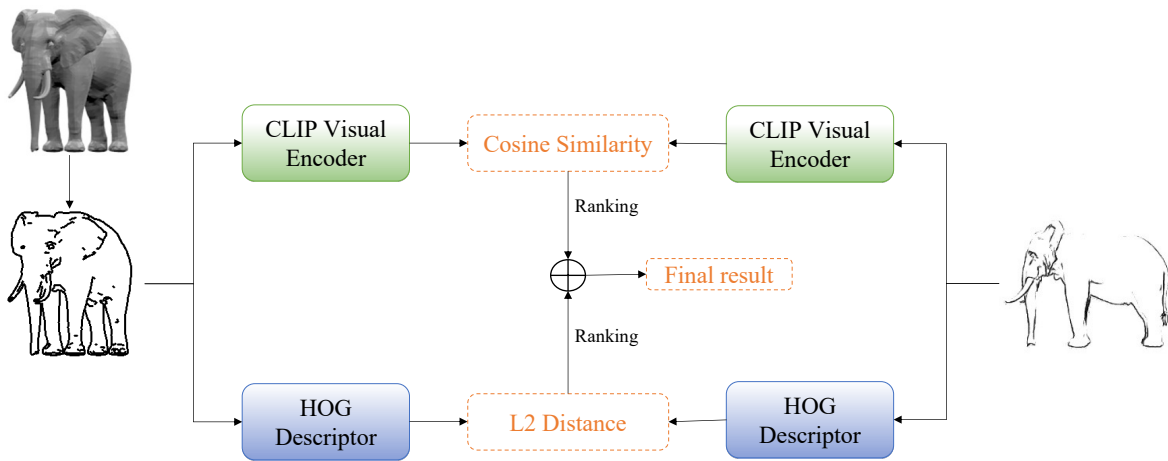
When they obtain the feature vectors of 3 rings, these vectors are passed into 2 T-encoder blocks to know which ring is useful for the model to learn the features of the current object.



(a) Proposed framework of TikTorch team.



(b) Proposed framework of Etinifni team.



(c) Proposed framework of THP team.

Fig. 3: Pipeline of contrastive learning frameworks used in the SketchANIMAR competition.

Then, the vectors are averaged to get the feature vector of the 3D object.

Embedding into common space. To compute the similarity between objects and sketches, their feature vectors are needed to embed into a common space. Feature vectors of 3D objects and sketches can have different dimensions so that two MLP networks with 2 layers having the same number of units in the output layer are used to bring them into the same vector space. Besides that, to avoid the overfitting effect, a Dropout layer [35] is added in each network. In the common space, the similarity between two embedding vectors \mathbf{u} and \mathbf{v} can be calculated using the cosine similarity metric:

$$\text{sim}(\mathbf{u}, \mathbf{v}) = \frac{\mathbf{u} \cdot \mathbf{v}}{\|\mathbf{u}\| \|\mathbf{v}\|} \quad (1)$$

Loss function. The contrastive loss function used is a customized version of Normalized Temperature-scaled Cross Entropy Loss (NT-Xent) [31]. Given a mini batch of $2N$ samples $\{\mathbf{x}_i\}_{i=1}^{2N}$ containing N objects and N sketches. They denote \mathbf{z}_i as the embedding vector of the sample \mathbf{x}_i in the common space. Let P_i be the set of indices of samples that are similar to \mathbf{x}_i in the current mini-batch exclusive of i , i.e. $(\mathbf{x}_i, \mathbf{x}_j)$ is a positive pair for $j \in P_i$. Here, \mathbf{x}_i can belong to many positive pairs, such as two 3D objects that are similar to the same sketch. The loss function for a positive pair $(\mathbf{x}_i, \mathbf{x}_j)$ is defined as:

$$l_{i,j} = -\log \frac{\exp(\text{sim}(\mathbf{z}_i, \mathbf{z}_j) / \tau)}{\sum_{k=1}^{2N} \mathbb{I}_{[k \neq i, k \notin P_i]} \exp(\text{sim}(\mathbf{z}_i, \mathbf{z}_k) / \tau)}, \quad (2)$$

where $\mathbb{I}_{[k \neq i, k \notin P_i]} \in \{0, 1\}$ is an indicator function evaluating to 1 if and only if $k \neq i$ and $k \notin P_i$, τ is a temperature parameter, $\text{sim}(\mathbf{u}, \mathbf{v})$ is the cosine similarity between two vectors \mathbf{u} and \mathbf{v} .

Training phase. During the training process, the optimizer used for training was AdamW [36], along with the StepLR algorithm to reduce the learning during the training process. They also applied the k -fold cross-validation technique with $k = 5$.

Retrieval phase. They ensemble the results of models trained on k -fold by max-voting. The similarity between a 3D object and a sketch image is the largest value of the similarity score computed by the 5 models.

5.2.2. Data Pre-Processing

Generation of multi-view images for 3D objects. Before generating batch images from 3D objects, it is essential to ensure axial synchronization of the objects so that the resulting multi-view images with their corresponding camera angles are consistent. To achieve this, they carefully examine the available dataset and identify several objects that are rotated at a 90-degree angle along the Ox axis. Then, they apply a consistent rotation to align these objects with the majority of the dataset as in Fig. 4.

Among seven rings, as in Fig. 2, they find that the most informative views are captured from rings 2, 3, and 4, which provide a 360-degree perspective around the object. Hence, they focus on processing the images from these rings to extract the relevant features and information.

To enhance the sketch-like appearance of the multi-view images, they utilize the Canny edge detector [37] to extract edge

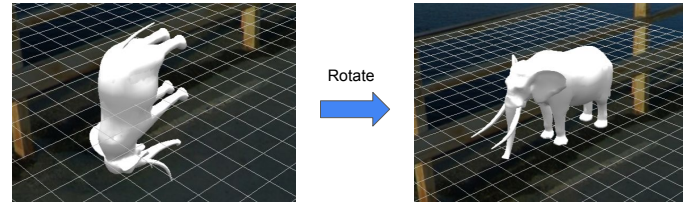


Fig. 4: Example of rotating a 3D object whose axis is not aligned with the majority of objects.

information. They also add some noises and variations to the edge information by randomly removing edges in the image using a traversal algorithm while preserving the underlying structure and content of the image (see Fig. 5). Figure 6 illustrates the outcome of the process of generating multi-view images for a 3D object.

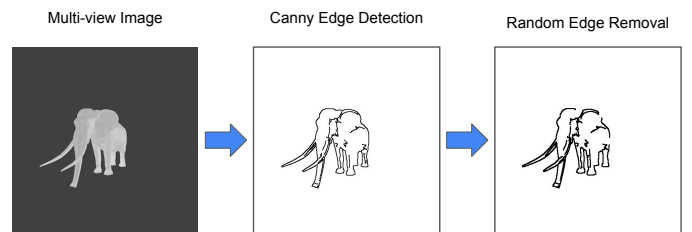


Fig. 5: Multi-view image processing steps.

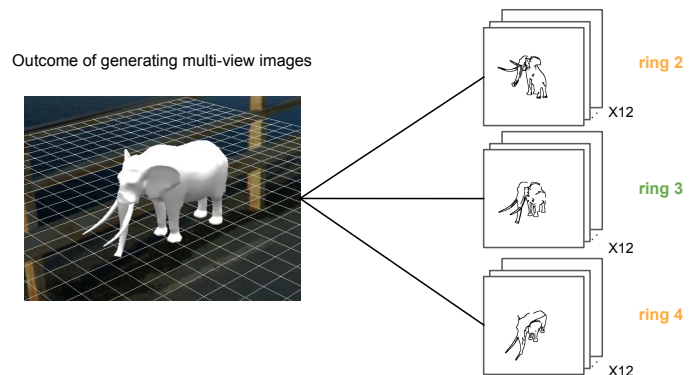


Fig. 6: Outcome of generating multi-view images for 3D objects. Each 3D object is represented by a set of 3 rings, and each ring is a collection of 12 images.

Generation of training sketch query images. Firstly, they cluster similar 3D objects together by some algorithms to check the similarity between the distribution of points in the point clouds and also the manual checking as post-processing. After that, they identify the best-quality object in each cluster, which usually is the most fine-grained object (i.e., the highest number of points in the point cloud). Then, when they generate a sketch-line image for each object in this cluster and use it for contrastive learning, they pick the image of the best-quality object as the representative sketch (depicted in Fig. 7).

To expand training samples for contrastive learning, they develop a method to generate three queries per object. Each query is randomly chosen from rings 2, 3, and 4 (see Fig. 2) with probabilities of 0.2, 0.6, and 0.2, respectively, as they observe

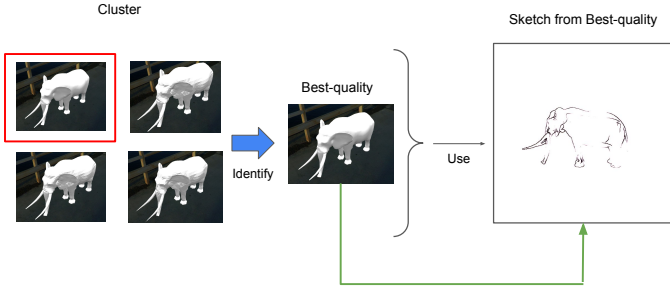


Fig. 7: Optimizing object sketches through clustering: the sketch of the best-quality object for all objects within a group of similar 3D objects is used.

that the majority of informative queries are in ring 3. Once a ring is selected, they randomly choose an image within that ring from the cluster this object belongs to and apply random Canny edge [37] or Artline [38] techniques, along with image horizontal flip and rotation transformations. By implementing this process, they are able to significantly increase the number of our training samples from about 100 samples to 2500 samples while maintaining a high level of quality.

5.3. THP Team

5.3.1. Architecture of Proposed Network

Figure 3c illustrates an overview of the proposed network. To evaluate the similarity of two given sketch images, they compare the distance of global features and local features and then combine the results.

To extract global features, they use the pre-trained CLIP model [39]. The input of CLIP model is the dilated Canny edge extracted from multi-view images. After that, CLIP feature vectors of view images and sketch queries are matched using cosine similarity. The final score is calculated as the maximum of scores of 4 views, in which each view score is calculated by the sum of the 6 highest similarities.

To increase local information awareness, they use the HOG descriptor [40] on both sketch and multi-view images. The HOG vectors are then matched using the L2 distance. They are also ranked like CLIP feature vectors.

Finally, they combine CLIP and HOG similarity scores as follows: $Score = \alpha * CLIP\ score + (1 - \alpha) * HOG\ score$, where $\alpha = 0.7$.

5.3.2. 2D Shape Projection

They use 4 camera setups to take multiple views of 3D objects:

- For the first camera setup, assuming the 3D object is initially solid along the z-axis, the camera is solid on the Oxy plane and looks at the center of the object. The camera is moved around the subject to create 12 views from a distance of 30 degrees each time.
- For the second camera setup, the camera is raised to 30 degrees above the Oxy plane and moved around to create the next 12 views.

- For the third camera setup, the camera is placed on the Oyz plane and looks at the center of the object. The camera is moved like the first camera setup to create the next 12 views.
- Camera for the last setup is raised from the third setup to 30 degrees to create the next 12 views.

There are a total of 48 views for each object. Note that it is possible to create images from other directions, but according to their tests, from these 48 views, they can observe the characteristics of objects.

5.3.3. Sketch Pre-processing

To reduce the domain gap, they apply Canny edge algorithm [37] for each 2D projection image to create an image similar to the sketch image because the sketch is also a special type of edge. Both sketch and Canny edge images are then cropped and resized to 224×224 with the padding of 5 pixels. After that, edges are further clarified using the dilation morphology algorithm. The sketch pre-processing pipeline is shown in Fig. 8.

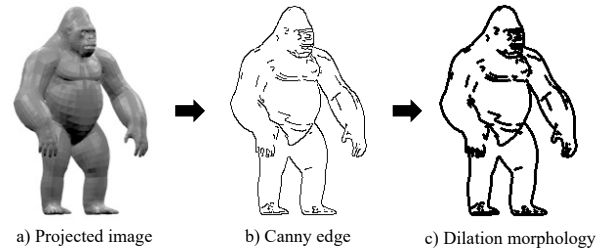


Fig. 8: Pipeline of sketch pre-processing.

5.4. Etinifni Team

5.4.1. Overview of Proposed Solution

Due to the nature of the retrieval tasks, they build a deep learning framework using the CLIP model [39] as the backbone. The framework performs the following steps:

1. Pre-process the dataset to re-direct the 3D objects into one single vertical orientation.
2. Extract multi-views (*i.e.*, 12 random views around the objects in uniform angles) from the 3D objects.
3. Encode the 2D sketches and the view images of 3D objects using the AutoEncoder that is built upon the ResNet50.
4. Reduce the size of the feature vectors from 512 to 128 through the projection head.
5. Compare feature vectors of sketches and the 3D objects using the cosine similarity function. After that, they can identify the matching pairs of sketches and 3D objects.

5.4.2. Data Pre-Processing

Resize objects: They resize the 3D objects to fit the 3D object inside an imaginary box of $2 \times 2 \times 2$ by re-scaling the dimensions (x, y, z) of the 3D objects into the new dimension (x', y', z') not greater than 2m using the following formula:

$$(x', y', z') = \left(\frac{2x}{\max(x, y, z)}, \frac{2y}{\max(x, y, z)}, \frac{2z}{\max(x, y, z)} \right) \quad (3)$$

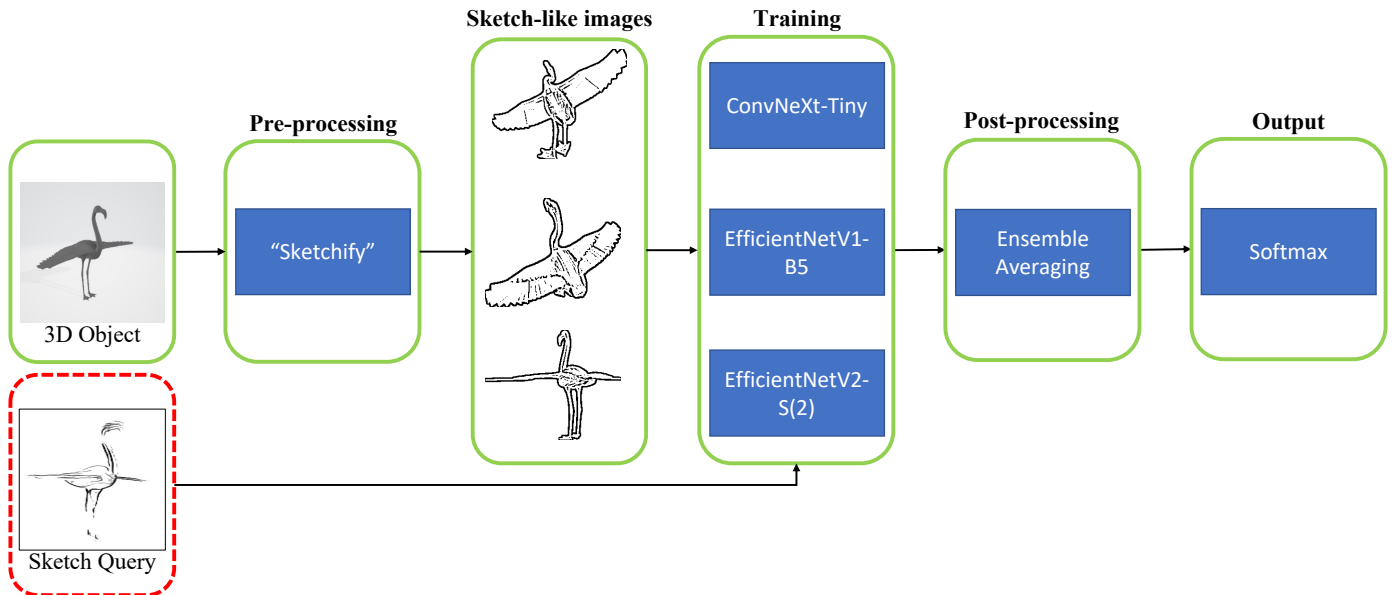


Fig. 9: Proposed framework of V1olet team.

Re-orientate objects: They re-direct the orientation of the 3D objects manually so that the 3D objects are standing (*i.e.*, the objects are in an erect position).

5.4.3. Multi-view Generation

They first rotate the camera as in Fig. 2. At each position, they apply 3D image rendering to provide a more accurate and detailed view of objects, enabling the model to extract the necessary features for retrieval with greater precision, even where subtle variations in shape and texture can be crucial in determining an object's identity. Models can then extract the most detailed and accurate information possible, leading to more robust and reliable results.

5.4.4. Data Augmentation

Due to the limited available training data, data augmentation techniques are applied to increase the number of training data:

Outline modifications:

- **Thickness:** is an important aspect of 2D objects as it determines the physical properties and functionality of the object. They adjust the thickness of the object edges, thereby generating new sketches with different lengths.
- **Geometry:** is an essential branch of mathematics that deals with the study of shapes, sizes, positions, and dimensions of objects in space. Here, they adjust the stroke of different zigzag edges.

Image processing:

- **Random deletion:** To ensure the robustness of the sketch, they partition the 2D images into multiple blocks. Each block is equal in size and contains a subset of pixels from the original image. They randomly select a portion of these blocks and removed them from the image to simulate missing strokes on the data set.

- **Image compression:** Because the provided query images are of low quality, a compressor is utilized to reduce the quality of images to breed the sketches.

View extraction:

- The camera is set up at a suitable distance, height, and orientation to ensure comprehensive coverage of the object's surface. The camera views are then randomly selected to capture a diverse set of angles for robust 3D reconstruction.

5.5. V1olet Team

5.5.1. Proposed Classification Approach

They formulate the retrieval task as a classical classification problem. Particularly, several potential CNNs, including EfficientNet [41], EfficientNetV2 [32], and ConvNeXt [42] are employed to recognize whether the sketch query and 3D objects are the same class. These networks are renowned for their remarkable feature extraction capabilities and are considered state-of-the-art in the domain of image recognition. The used models also are lightweight and suitable for real-life applications while achieving considerable performance.

Ensemble Solution. Figure 9 illustrates the proposed ensemble approach by averaging the predictions of each model. This approach effortlessly helps to mitigate the potential shortcomings of individual models, resulting in improved performance and robust generalization to varying data distributions.

To further improve accuracy of models, they also utilize Test Time Augmentation (TTA), which involves applying a range of transformations such as rotations, flips, and translations to test images and averaging the results to obtain the final prediction. Specifically, they utilize horizontal flipping to provide additional perspectives of the original images. This technique not only enhances generalization but also enables the model to

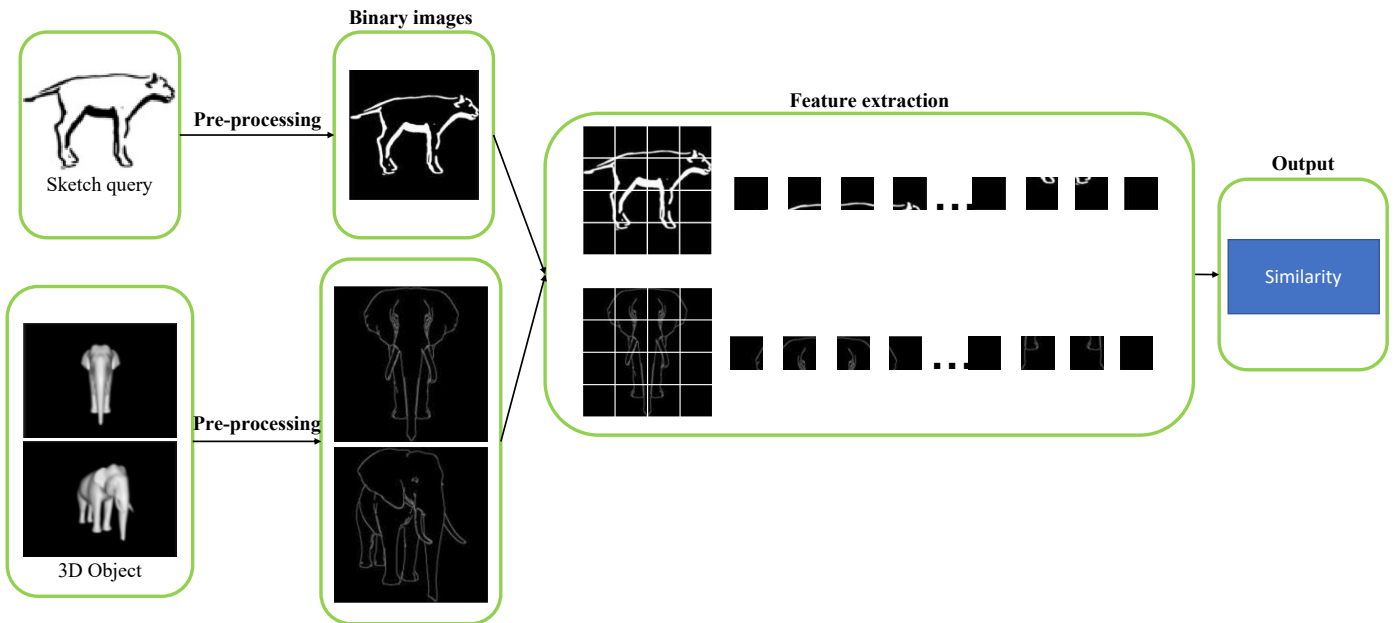


Fig. 10: Proposed framework of DH team.

recognize objects that may be oriented differently from those in the training set.

Training Phase. To evaluate the performance of used models, they created a validation set by randomly leaving out 10% of samples from each class in the training data. Pre-trained models on ImageNet were fine-tuned using the remaining training sets. They also employed the cross-entropy loss with label smoothing of 0.1 to prevent overfitting and improve the generalizability of models. Sketchified multi-view images were jointly trained with the original sketch queries to enforce networks to recognize them as the same class. During both training and inference, an image size of 384×384 was utilized. All networks were trained for 20 epochs using the Adam optimizer [43] with a learning rate of 0.0001. Finally, they selected the models with the best validation accuracy for ensembling.

Retrieval Phase. Given a sketch query, the ensemble averaging of CNN models produces a set of softmax probabilities. These probabilities are then used to identify whether the sketch query and sketch-like images generated from the 3D object belong to the same class. The softmax probabilities also serve as a ranking metric, which allows for the sorting of the retrieved 3D objects by relevance.

5.5.2. Data Pre-processing

Figure 11 demonstrates an overview of the proposed data pre-processing pipeline. In general, it can be divided into three steps: Ringview extraction, color reversal, and sketchify.

Ringview extraction. Extracting multiple views of an object can be highly advantageous for various applications, including 3D object retrieval. They extract multiple views from 7 rings with 12 views on each ring like Fig. 2. By providing different perspectives of the 3D object, these multiple views can be used to extract more robust and detailed features to train models with greater accuracy for 3D object retrieval. Thus, ringview

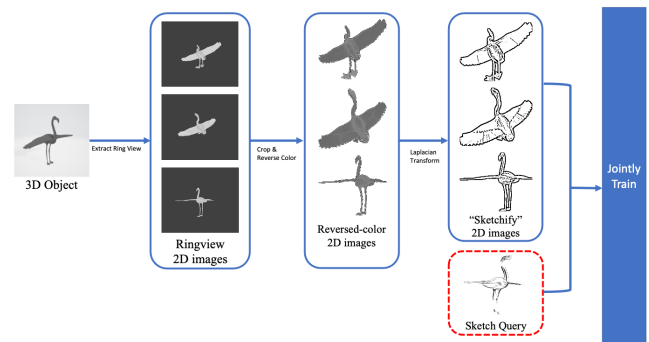


Fig. 11: The proposed data pre-processing pipeline

processing is a useful technique that can improve the accuracy of models for 3D object retrieval.

Color reversal. It is also crucial to consider the background of the images when matching 3D objects with the querying sketches. Typically, these sketches usually have a white background, while the multiple 2D images obtained from the ringview extraction step have a grey background. To solve this problem, they merely flip the color of the ringview image, making the backdrop translucent to match the background of the target sketch queries. Therefore, the resulting images better resemble the sketch queries and hence, support the further "sketchify" procedure.

Sketchify. Laplacian Transform is utilized to produce images that are more similar to sketches. Particularly, the Laplacian Transform, as a linear operator, is applied to the gray-scale image to generate a second-order derivative image that enhances the edges and transitions of the image [44]. The operator produces a sketch-like version of an image by thresholding the Laplacian image to obtain a binary edge map, which is used

to synthesize a sketch-like representation of the image. This transformation enables more efficient comparison of the views with the sketch query, as the critical matching features become more pronounced, facilitating accurate matching.

5.6. DH Team

5.6.1. Proposed Method

They propose a simple method to measure the distance between 2 images with fast execution speed due to the small number of computations. Based on the observation that 3D objects with the same shape will have the same distribution of pixels in 2D projection space, they propose the idea of dividing the image into small parts and then comparing each area to measure the similarity between the two images. Figure 10 shows the proposed framework, including four main modules: 2D sketch processing, 3D model processing, image feature extraction, and feature matching.

2D sketch processing. They crop images with the goal of keeping only the part containing the animals and removing the background. Since sketches in the dataset only contain the animal and no other extraneous details in the background, they define the animal’s bounding box as follows: First, sketches are converted to binary images and then inverted. Then they find the top line and the bottom image line with the value 255, these two lines correspond to the top and bottom edges of the bounding box; the same method is applied for the left and right edges. After that, they crop the part containing the animal into square with the size of a maximum of bounding-box height and width and then resize the image to 224×224 .

3D model processing. They first rotate the 3D objects using the Open3D library and capture the 3D model from 21 different perspective views. After that, view images are cropped similarly to 2D sketches.

Image feature extraction. The images are divided into 4×4 squares, and then the ratio of total pixel values in each square to total pixel values of the whole image is considered at the score of the square. At the end of this step, a 16-dimensional feature vector represents an image, including the sketch image and the view image.

Feature matching. Given a sketch query image Q and a 3D model R . After extracting features, they obtain f^Q representing the sketch image and $f_i^R, i = 1..21$ representing 21 view images corresponding to the 3D model. The similarity score between the sketch query Q and the 3D model R is defined as:

$$D(Q, R) = \min \|f^Q - f_i^R\|_2. \quad (4)$$

6. Results and Discussions

Our SketchANIMAR track involves the assessment of submitted runs on two subsets, namely the public test and the private test. The private test was comprised of 66 sketch queries, which corresponded to 265 query-model pairs. To prevent any potential cheating, about half of the private test (30 sketch queries) was randomly extracted and designated as the public test. The leaderboard for the private test was only unveiled post the conclusion of the challenge.

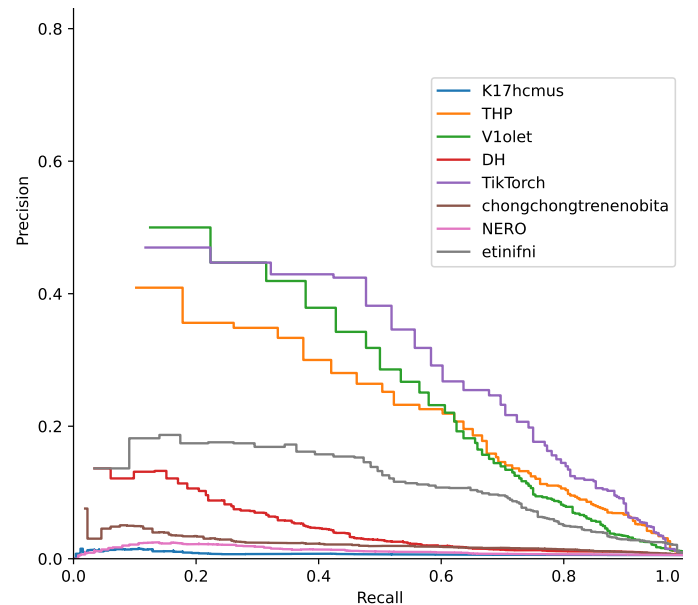


Fig. 12: The visualization of precision-recall curves of submissions on the private test of teams. It can be seen that TikTorch team achieves the best average performance with the highest area under the curve, while V1olet obtains the top precision at low recall (recall ≤ 0.2) among the eight teams. These insights are compatible with results in Table 2a, TikTorch and V1olet secure top 1 position in terms of mAP and NN, respectively.

Table 2 presents the leaderboard outcomes for both the public test and the private test. It is noteworthy that only the best-performing runs submitted by each team are shown. Nevertheless, for a fair comparison, we analyze only results on the private test, which evaluated all submitted sketch queries.

As seen in Table 2a, the TikTorch and V1olet team’s presented methods repeatedly stood out as the top effective strategies. On 3 out of 4 performance metrics (P@10, NDCG, and mAP), TikTorch outperformed rival teams by a wide margin. In terms of NN metric, the V1olet team secured the top 1 position. Meanwhile, THP took up the third position, both on public and private leaderboards. Most of the teams achieving high performances apply the view-base approach, which analyzes shape features from a set of 2D view projections. For the public test, similar findings are also shown in Table 2b. The first two teams TikTorch and V1olet achieve the top two ranks. In contrast, the performance of the other four teams (*i.e.*, THP, Etinifni, and DH) is constant across test sets, both private and public. The findings suggest that there is still opportunity for progress in this research topic.

Figure 12 illustrates the precision-recall curves of submissions on the private test of eight teams including TikTorch, V1olet, THP, Etinifni, DH, Chongchongtrenenobita, Nero, and K17hcmus, respectively. It is clear that among the eight teams, TikTorch team has the best average performance with the biggest area under the curve, while V1olet has the maximum precision at low recall (recall ≤ 0.2). These conclusions are consistent with Table 2a’s findings, which show that TikTorch and V1olet both rank first in terms of mAP and NN. Furthermore, the precision-recall curves of three team TikTorch, V1olet, and THP share the similar shape, which show the effec-

Table 2: Leaderboard results of SketchANIMAR competition.

Team	NN	P@10	NDCG	mAP	Team	NN	P@10	NDCG	mAP
TikTorch	0.470 (2)	0.255 (1)	0.669 (1)	0.522 (1)	TikTorch	0.533 (1)	0.280 (1)	0.708 (1)	0.570 (1)
Violet	0.500 (1)	0.232 (2)	0.640 (2)	0.453 (2)	Violet	0.467 (2)	0.213 (2)	0.613 (2)	0.411 (2)
THP	0.409 (3)	0.226 (3)	0.608 (3)	0.421 (3)	THP	0.433 (3)	0.207 (3)	0.601 (3)	0.399 (3)
Etinifni	0.136 (4)	0.158 (4)	0.473 (4)	0.274 (4)	Etinifni	0.200 (4)	0.147 (4)	0.489 (4)	0.303 (4)
DH	0.136 (4)	0.088 (6)	0.372 (6)	0.158 (6)	DH	0.100 (5)	0.080 (5)	0.361 (6)	0.140 (6)
Chongchong...	0.076 (5)	0.045 (7)	0.300 (7)	0.079 (7)	Chongchong...	0.067 (6)	0.053 (6)	0.307 (7)	0.081 (7)
Nero	0.000 (6)	0.009 (9)	0.240 (8)	0.038 (8)	K17hcmus	0.000 (7)	0.027 (7)	0.241 (9)	0.044 (8)
K17hcmus	0.000 (6)	0.014 (8)	0.223 (9)	0.029 (9)	Nero	0.000 (7)	0.007 (8)	0.248 (8)	0.041 (9)

(a) Best run results on the private test.

(b) Best run results on the public test.

tiveness at low recall threshold (recall ≤ 0.4) but drop significantly at high one (recall ≥ 0.8).

In conclusion, the view-based learning method has proven to be an effective strategy for reaching high performance. The difficulty of feature extraction models [45, 46] can be attributed to the high point cloud density of the 3D objects in the ANIMAR dataset. It's important to remember that these models often randomly sample a certain number of cloud points (*e.g.*, 1024, for example). Contrarily, by utilizing the semantic data and representation of 3D objects, the use of view pictures obtained by moving the trajectory camera, as demonstrated in Fig. 2, enhances feature learning. This further demonstrates the effectiveness of the view-based learning strategy for retrieving 3D objects.

7. Conclusion

This paper introduces a novel track for sketch-based retrieval of fine-grained 3D animal models, along with a newly constructed ANIMAR dataset. Our SHREC 2023 challenge track is designed to simulate real-life scenarios and requires participants to retrieve 3D animal models based on complex and detailed sketches. The challenge received submissions from eight teams, resulting in a total of 204 runs with different approaches. The evaluated results of this track were satisfactory but also revealed the difficulties of the task at hand.

In future research, we aim to expand the dataset by collecting a more diverse range of 3D animal models that encompass a wider variety of species, environmental contexts, and postures. This can enhance the generalization capability of potential solutions and improve performance on unseen 3D animal models. Additionally, we intend to generate synthetic data and texture to augment 3D animal models with different postures, backgrounds, and patterns to train more effective and robust representation models. We believe that by exploring these research avenues, we can advance the state-of-the-art in 3D object retrieval.

CRedit authorship contribution statement

Trung-Nghia Le: Conceptualization, Writing – review & editing, Project administration, Supervision. **Tam V. Nguyen:** Conceptualization, Writing – review & editing. **Minh-Quan Le:** Software, Writing – review & editing. **Trong-Thuan**

Nguyen: Software, Writing – review & editing. **Viet-Tham Huynh:** Data curation. **Trong-Le Do:** Software, Investigation. **Khanh-Duy Le:** Visualization. **Mai-Khiem Tran:** Data curation. **Nhat Hoang-Xuan:** Software. **Thang-Long Nguyen-Ho:** Software. **Vinh-Tiep Nguyen:** Conceptualization. **Nhat-Quynh Le-Pham:** Methodology, Writing – original draft. **Huu-Phuc Pham:** Methodology, Writing – original draft. **Trong-Vu Hoang:** Methodology, Writing – original draft. **Quang-Binh Nguyen:** Methodology, Writing – original draft. **Hai-Dang Nguyen:** Methodology, Writing – original draft. **Trong-Hieu Nguyen-Mau:** Methodology, Writing – original draft. **Tuan-Luc Huynh:** Methodology, Writing – original draft. **Thanh-Danh Le:** Methodology, Writing – original draft. **Ngoc-Linh Nguyen-Ha:** Methodology, Writing – original draft. **Tuong-Vy Truong-Thuy:** Methodology, Writing – original draft. **Truong Hoai Phong:** Methodology, Writing – original draft. **Tuong-Nghiem Diep:** Methodology, Writing – original draft. **Khanh-Duy Ho:** Methodology, Writing – original draft. **Xuan-Hieu Nguyen:** Methodology, Writing – original draft. **Thien-Phuc Tran:** Methodology, Writing – original draft. **Tuan-Anh Yang:** Methodology, Writing – original draft. **Kim-Phat Tran:** Methodology, Writing – original draft. **Nhu-Vinh Hoang:** Methodology, Writing – original draft. **Minh-Quang Nguyen:** Methodology, Writing – original draft. **Hoai-Danh Vo:** Methodology, Writing – original draft. **Minh-Hoa Doan:** Methodology, Writing – original draft. **Ak-ihiro Sugimoto:** Conceptualization. **Minh-Triet Tran:** Conceptualization, Supervision, Funding acquisition, Writing - Review & Editing.

Data availability

Data will be made available upon request.

Declaration of competing interest

The authors declare that they have no known competing financial interests or personal relationships that could have appeared to influence the work reported in this paper.

Acknowledgments

This work was funded by the Vingroup Innovation Foundation (VINIF.2019.DA19) and National Science Foundation Grant (NSF#2025234).

References

- [1] Stotko, P, Krumpfen, S, Hullin, MB, Weinmann, M, Klein, R. Slamcast: Large-scale, real-time 3d reconstruction and streaming for immersive multi-client live telepresence. *IEEE transactions on visualization and computer graphics* 2019;25(5):2102–2112.
- [2] Liu, X, Kofman, J. Real-time 3d surface-shape measurement using background-modulated modified fourier transform profilometry with geometry-constraint. *Optics and Lasers in Engineering* 2019;115:217–224.
- [3] Wang, J, Mueller, F, Bernard, F, Sorli, S, Sotnychenko, O, Qian, N, et al. Rgb2hands: real-time tracking of 3d hand interactions from monocular rgb video. *ACM Transactions on Graphics (ToG)* 2020;39(6):1–16.
- [4] Guo, H, Peng, S, Lin, H, Wang, Q, Zhang, G, Bao, H, et al. Neural 3d scene reconstruction with the manhattan-world assumption. In: *Proceedings of the IEEE/CVF Conference on Computer Vision and Pattern Recognition*. 2022, p. 5511–5520.
- [5] Yookwan, W, Chinnsarn, K, So-In, C, Horkaew, P. Multimodal fusion of deeply inferred point clouds for 3d scene reconstruction using cross-entropy icp. *IEEE Access* 2022;10:77123–77136.
- [6] Li, J, Gao, W, Wu, Y, Liu, Y, Shen, Y. High-quality indoor scene 3d reconstruction with rgb-d cameras: A brief review. *Computational Visual Media* 2022;8(3):369–393.
- [7] Gümeli, C, Dai, A, Nießner, M. Roca: robust cad model retrieval and alignment from a single image. In: *Proceedings of the IEEE/CVF Conference on Computer Vision and Pattern Recognition*. 2022, p. 4022–4031.
- [8] Manda, B, Kendre, PP, Dey, S, Muthuganapathy, R. Sketchcleanet—a deep learning approach to the enhancement and correction of query sketches for a 3d cad model retrieval system. *Computers and Graphics* 2022;107:73–83.
- [9] Salihi, D, Steinbach, E. Sgpcr: Spherical gaussian point cloud representation and its application to object registration and retrieval. In: *Proceedings of the IEEE/CVF Winter Conference on Applications of Computer Vision*. 2023, p. 572–581.
- [10] Koca, BA, Çubukçu, B, Yüzgeç, U. Augmented reality application for preschool children with unity 3d platform. In: *2019 3rd International Symposium on Multidisciplinary Studies and Innovative Technologies (ISMSIT)*. IEEE; 2019, p. 1–4.
- [11] Guo, C, Jiang, T, Chen, X, Song, J, Hilliges, O. Vid2avatar: 3d avatar reconstruction from videos in the wild via self-supervised scene decomposition. *arXiv preprint arXiv:230211566* 2023;.
- [12] Nie, W, Ninh, VT, Su, Y, Ton-That, V, Tran, MT, Xiang, S, et al. Shrec'18 track: 2d scene sketch-based 3d scene retrieval. *Training* 2018;18:70.
- [13] Yuan, J, Abdul-Rashid, H, Li, B, Lu, Y, Schreck, T, Bui, NM, et al. Shrec'19 track: Extended 2d scene sketch-based 3d scene retrieval. *Training* 2019;18:70.
- [14] Qin, J, Yuan, S, Chen, J, Ben Amor, B, Fang, Y, Hoang-Xuan, N, et al. Shrec'22 track: Sketch-based 3d shape retrieval in the wild. *Computers and Graphics* 2022;.
- [15] Abdul-Rashid, H, Yuan, J, Li, B, Lu, Y, Bai, S, Bai, X, et al. 2D Image-Based 3D Scene Retrieval. In: Telea, A, Theoharis, T, Veltkamp, R, editors. *Eurographics Workshop on 3D Object Retrieval*. 2018;.
- [16] Abdul-Rashid, H, Yuan, J, Li, B, Lu, Y, Schreck, T, Bui, NM, et al. Shrec'19 track: Extended 2d scene image-based 3d scene retrieval. *Eurographics Workshop on 3D Object Retrieval* 2019;700:70.
- [17] Li, W, Liu, A, Nie, W, Song, D, Li, Y, Wang, W, et al. Shrec 2019-monocular image based 3d model retrieval. In: *Eurographics Workshop 3D Object Retrieval*. 2019, p. 1–8.
- [18] Li, W, Song, D, Liu, A, Nie, W, Zhang, T, Zhao, X, et al. SHREC 2020 Track: Extended Monocular Image Based 3D Model Retrieval. In: Schreck, T, Theoharis, T, Pratikakis, I, Spagnuolo, M, Veltkamp, RC, editors. *Eurographics Workshop on 3D Object Retrieval*. 2020;.
- [19] Feng, Y, Gao, Y, Zhao, X, Guo, Y, Bagewadi, N, Bui, NT, et al. Shrec'22 track: Open-set 3d object retrieval. *Computers & Graphics* 2022;107:231–240.
- [20] Yuan, J, Li, B, Lu, Y, Bai, S, Bai, X, Bui, NM, et al. Shrec'18 track: 2d scene sketch-based 3d scene retrieval. *Eurographics Workshop on 3D Object Retrieval* 2018;18:70.
- [21] Yuan, J, Abdul-Rashid, H, Li, B, Lu, Y, Schreck, T, Bui, NM, et al. Shrec'19 track: Extended 2d scene sketch-based 3d scene retrieval. *Eurographics Workshop on 3D Object Retrieval* 2019;18:70.
- [22] Furuya, T, Ohbuchi, R. Deep aggregation of local 3d geometric features for 3d model retrieval. In: *Proceedings of the British Machine Vision Conference (BMVC)*. 2016;.
- [23] Wang, PS, Liu, Y, Guo, YX, Sun, CY, Tong, X. O-cnn: Octree-based convolutional neural networks for 3d shape analysis. *ACM Trans Graph* 2017;.
- [24] Wang, W, Shen, J, Porikli, F. Saliency-aware geodesic video object segmentation. In: *CVPR*. 2015, p. 3395–3402.
- [25] Xie, S, Girshick, R, Dollár, P, Tu, Z, He, K. Aggregated residual transformations for deep neural networks. In: *CVPR*. 2017, p. 1492–1500.
- [26] Su, H, Maji, S, Kalogerakis, E, Learned-Miller, EG. Multi-view convolutional neural networks for 3d shape recognition. In: *ICCV*. 2015;.
- [27] Savva, M, Yu, F, Su, H, Kanezaki, A, Furuya, T, Ohbuchi, R, et al. Shrec'17 track large-scale 3d shape retrieval from shapenet core55. In: *Proceedings of the Workshop on 3D Object Retrieval*. 2017;.
- [28] Moscoso Thompson, E, Biasotti, S, Giachetti, A, Tortorici, C, Werghe, N, Obeid, AS, et al. Shrec 2020: Retrieval of digital surfaces with similar geometric reliefs. *Computers and Graphics* 2020;.
- [29] Wu*, Y, Chen*, Z, Liu, S, Ren, Z, Wang, S. CASA: Category-agnostic skeletal animal reconstruction. In: *Neural Information Processing Systems*. 2022;.
- [30] Douze, M, Tolias, G, Pizzi, E, Papakipos, Z, Chausson, L, Radenovic, F, et al. The 2021 image similarity dataset and challenge. *arXiv preprint arXiv:210609672* 2021;.
- [31] Chen, T, Kornblith, S, Norouzi, M, Hinton, G. A simple framework for contrastive learning of visual representations. In: *International conference on machine learning*. 2020, p. 1597–1607.
- [32] Tan, M, Le, Q. Efficientnetv2: Smaller models and faster training. In: *International conference on machine learning*. 2021, p. 10096–10106.
- [33] Russakovsky, O, Deng, J, Su, H, Krause, J, Satheesh, S, Ma, S, et al. ImageNet Large Scale Visual Recognition Challenge. *International Journal of Computer Vision* 2015;115(3):211–252.
- [34] Vaswani, A, Shazeer, N, Parmar, N, Uszkoreit, J, Jones, L, Gomez, AN, et al. Attention is all you need. *Advances in neural information processing systems* 2017;30.
- [35] Hinton, GE, Srivastava, N, Krizhevsky, A, Sutskever, I, Salakhutdinov, RR. Improving neural networks by preventing co-adaptation of feature detectors. *arXiv preprint arXiv:12070580* 2012;.
- [36] Loshchilov, I, Hutter, F. Decoupled weight decay regularization. *arXiv preprint arXiv:171105101* 2017;.
- [37] Canny, J. A computational approach to edge detection. *IEEE T-PAMI* 1986;(6):679–698.
- [38] Madhavan, V. Artline. <https://github.com/vijishmadhavan/ArtLine>; 2021. [Online; accessed 15-March-2023].
- [39] Radford, A, Kim, JW, Hallacy, C, Ramesh, A, Goh, G, Agarwal, S, et al. Learning transferable visual models from natural language supervision. In: *International conference on machine learning*. 2021, p. 8748–8763.
- [40] Dalal, N, Triggs, B. Histograms of oriented gradients for human detection. In: *CVPR*. 2005, p. 886–893.
- [41] Tan, M, Le, Q. Efficientnet: Rethinking model scaling for convolutional neural networks. In: *International conference on machine learning*. 2019, p. 6105–6114.
- [42] Liu, Z, Mao, H, Wu, CY, Feichtenhofer, C, Darrell, T, Xie, S. A convnet for the 2020s. In: *Conference on Computer Vision and Pattern Recognition*. 2022, p. 11976–11986.
- [43] Kingma, DP, Ba, J. Adam: A method for stochastic optimization. *arXiv preprint arXiv:14126980* 2014;.
- [44] Nealen, A, Sorkine, O, Alexa, M, Cohen-Or, D. A sketch-based interface for detail-preserving mesh editing. In: *ACM SIGGRAPH*. 2005, p. 1142–1147.
- [45] Qi, CR, Su, H, Mo, K, Guibas, LJ. Pointnet: Deep learning on point sets for 3d classification and segmentation. In: *Conference on Computer Vision and Pattern Recognition*. 2017, p. 652–660.
- [46] Muzahid, A, Wan, W, Sohel, F, Wu, L, Hou, L. Curvenet: Curvature-based multitask learning deep networks for 3d object recognition. *IEEE/CAA Journal of Automatica Sinica* 2020;8(6):1177–1187.